



Obrabotka metallov -

Metal Working and Material Science

Journal homepage: http://journals.nstu.ru/obrabotka_metallov



Study of the effect of a combined modifier from silicon production waste on the properties of gray cast iron

Antonina Karlina^{1, a, *}, *Viktor Kondratiev*^{2, b}, *Ivan Sysoev*^{3, c}, *Aleksandr Kolosov*^{4, d},
Marina Konstantinova^{3, e}, *Elena Guseva*^{3, f}

¹ National Research Moscow State University of Civil Engineering, 26 Yaroslavskoe Shosse, Moscow, 129337, Russian Federation

² A.P. Vinogradov Institute of Geochemistry of the Siberian Branch of the Russian Academy of Sciences, 1A Favorsky str., Irkutsk, 664033, Russian Federation

³ Irkutsk National Research Technical University, 83 Lermontova str., Irkutsk, 664074, Russian Federation

⁴ JSC Eurosibenergo, 22 Rabochaya str., Irkutsk, 664007, Russian Federation

^a  <https://orcid.org/0000-0003-3287-3298>,  karlinat@mail.com; ^b  <https://orcid.org/0000-0002-7437-2291>,  imz@mail.ru;

^c  <https://orcid.org/0000-0002-8561-5383>,  iwansys@mail.ru; ^d  <https://orcid.org/0000-0002-2330-1813>,  akolosov.irk@gmail.com;

^e  <https://orcid.org/0000-0002-8533-0214>,  mavikonst@mail.ru; ^f  <https://orcid.org/0000-0002-8719-7728>,  el.guseva@rambler.ru

ARTICLE INFO

Article history:

Received: 12 December 2023

Revised: 10 January 2024

Accepted: 22 January 2024

Available online: 15 March 2024

Keywords:

Modifiers

Grey cast iron

Nanostructures

Silicon dioxide

Morphology

Oxides

Crystallization

Plate

Compacted

Vermicular graphite

ABSTRACT

Introduction. During the metallurgical production of silicon, waste is generated that accumulates in dumps, harming the environment. Disposal and recycling of solid waste from silicon production is especially important because it contains important chemical compounds (silicon dioxide, silicon carbide, carbon nanotubes) that can be used in other industries, which will bring greater economic value. Considering the possibilities for extracting these useful components from silicon production waste, it is necessary to bring processing technologies to the stage of widespread practical application. Therefore, the development of a special waste processing technology to obtain a useful product in the form of a composition of silicon dioxide and silicon carbide remains an urgent problem. **The purpose of the work** is to study the formation of the morphological form of graphite when adding nano-modifiers from silicon production waste. **Methods.** The work examined specimens of gray cast iron after modification with a combined modifier obtained from silicon production waste. The research methods are mechanical tests for statistical tension, analysis of the chemical composition and metallographic studies. **Results and Discussion.** It is revealed that the mechanical properties of gray cast iron increased by 30–50 % after modification with a combined modifier, compared with witness specimens. The morphology of graphite is an important parameter affecting the properties of cast iron. It is established that during the modification process the morphology of graphite changes from lamellar to vermicular. Specimens of gray cast iron with vermicular form of graphite have high strength values compared to specimens of gray cast iron with lamellar form of graphite. The presented results confirm the prospects of the developed approach aimed at obtaining new classes of modifiers and products made of gray cast iron with a high complex of mechanical properties.

For citation: Karlina A.I., Kondratiev V.V., Sysoev I.A., Kolosov A.D., Konstantinova M.V., Guseva E.A. Study of the effect of a combined modifier from silicon production waste on the properties of gray cast iron. *Obrabotka metallov (tekhnologiya, oborudovanie, instrumenty)* = *Metal Working and Material Science*, 2024, vol. 26, no. 1, pp. 194–211. DOI: 10.17212/1994-6309-2024-26.1-194-211. (In Russian).

Introduction

A large amount of waste is generated during the operation of steel plants around the world. Typically, this solid waste is partially recycled, but a significant amount remains, causing damage to the environment. In all technological processes for the production of metallic silicon, material losses of varying degrees and quality occur. In Russia, at silicon production plants, a lot of unprocessed metallurgical slag remains in

* Corresponding author

Karlina Antonina I., Ph.D. (Engineering), Research Associate
 National Research Moscow State Construction University,
 Yaroslavskoe shosse, 26,
 129337, Moscow, Russia
 Tel: +7 950 120-19-50, e-mail: karlinat@mail.ru

the dumps [1, 2]. Storage of this solid waste requires many square kilometers of land. Waste is collected in the form of wet or dry powders [1–7]. It is estimated [1, 2, 6, 7] that more than 100,000 tons of waste are generated annually during the production of metallic silicon [7]. Despite significant efforts to reduce its harmful effects on the environment, there is no way to prevent contamination of soil and groundwater. Currently, work is being carried out in the Russian Federation on the use of industrial waste as modifying additives in various industries: construction [4–6], metallurgy [1, 2, 7].

Modification is one of the most important metallurgical treatments applied to molten iron immediately before casting to promote solidification without excessive eutectic undercooling, which promotes the formation of carbides, usually with undesirable graphite morphology. Gray iron (lamellar graphite) continues to be the most produced metal material in the global foundry industry, although its rate has slowed due to its replacement by higher-performing malleable irons or lighter-weight aluminum-based alloys.

It is well known [8–21] that the crystallization of graphite is significantly influenced by the presence of molten impurities in the melt in which it grows, even when these minor elements are present in quantities of less than 0.1 %. It can have a positive effect, promoting nucleation and spheroidization, or a negative effect, causing graphite degeneration. The main source of these elements is charge materials such as scrap steel, pig iron and pig iron return. A three-stage model of the nucleation of lamellar graphite in gray cast iron was proposed in 2,000 with the formation of oxide-sulfide graphite [8–14]. A large series of research programs have defined the following model [8–21]:

- (1) Small oxide regions ($0.1\text{--}3\ \mu\text{m}$, typically $< 2\ \mu\text{m}$) are formed in the melt;
- (2) Complex compounds $(Mn,X)S$ (from 1 to $10\ \mu\text{m}$, usually $< 5\ \mu\text{m}$) nucleate on these microinclusions, where $X = Ca, Ba, Sr, Zr, Mg, P, Ti, La, Ce$, etc.;
- (3) Graphite nucleates on the sides of $(Mn,X)S$ compounds due to the low crystallographic mismatch of graphite [8, 9].

The role of complex sulfides $(Mn,X)S$ in the formation of graphite in gray cast irons is confirmed by other representative research works [10–15]. Recently [16, 17] it was discovered that oxygen is mainly present in the first microcompound, which is visible as the core of the $(Mn,X)S$ particle, and, in any case, also at the sulfide-graphite interface, formed into a thin (nano-sized) layer and including $O, Si, Al, Ca, Ba, Sr, La$ and Mg . The presence of this oxide-based layer is hypothesized to increase the ability of $(Mn,X)S$ compounds to nucleate graphite due to their better crystallographic compatibility: this is illustrated by the use of a hexagonal system compared to a cubic system for sulfide and the low mismatch found for the face (0001) graphite. The smaller the mismatch between two substances (δ), the stronger the nucleation potential between it: the highest nucleation capacity is achieved at $\delta < 6\%$ ($LaS, CeS, SrMnS$), the average nucleation capacity is achieved at $\delta = 6\%$ to 12% (BaS, CaS), and weak nucleation ability is detected at $\delta > 12\%$ (MnS, MgS) [18, 19]. The results of research on the morphological characteristics of graphite lead to adjustments to national standards [22–25].

The works [1, 2, 7] show the possibility of using silicon production waste as modifiers in the production of cast iron. Two modifiers were developed [7], obtained after flotation processing of waste in the form of silicon dioxide and nanotubes [1, 7]. The use of modifiers obtained from silicon production waste not only improves the mechanical properties of gray cast iron, but also affects the morphology of graphite [26–34]. The morphology of graphite is a very important parameter affecting the properties of cast iron. The room temperature morphology of graphite in cast $Fe\text{-}C\text{-}Si$ alloys is primarily the result of nucleation from a liquid melt and growth of graphite crystals followed by diffusive growth of carbon in the solid state. The chemical complexity of iron melts and the temporary nature of nucleation and local segregation caused by the chemical composition of the alloy, melt processing and casting conditions are the main determining factors. The interaction between these variables can result in a wide variety of graphite forms, including lamellar/flake (LG), compacted/vermicular (CG), spheroidal/nodular (SG), and other graphite forms (TG) [9, 10, 14, 15, 26–9], as well as some degenerate morphologies such as pointed, blasted or massive graphite (CHG). Although nodular cast iron was discovered in the late 1930s [8–12], the mechanism, by which graphite changes its shape, remains unclear [8–21, 26–30]. Compacted graphite (CG) iron is a new engineering material containing graphite, worm-shaped (vermicular) with rounded edges in a (ferrite-pearlite) matrix.

In foreign literature the names compacted, vermicular, worm-shaped [22, 23, 25] can be found. In the domestic literature the term vermicular is used [24]. The intermediate graphite (*CG*) morphology provided an advantageous combination of the mechanical properties of ductile iron and the physical properties of gray cast iron.

The purpose of this work is to identify the formation of the morphological form of graphite with the introduction of a combined modifier from silicon production waste. **The objectives of the work are:**

- 1) to conduct research to assess the modifying effect of a combined modifier obtained from silicon production waste in the smelting of gray cast iron;
- 2) to determine the effect of the combined modifier on the nucleation of vermicular graphite;
- 3) to analyze the effects of compression/expansion during the crystallization of cast iron when using a combined modifier.

Experimental technique

Experimental cast iron (type *SCh15*) was smelted in an electric induction furnace (15 kg; 8,000 Hz) using cast iron scrap, *FeSi* and carbonaceous material. The melt, heated to 1,500 °C and held in the oven for 5 minutes, was released into a pouring ladle at a temperature of 1,480 °C and poured into a sand mold made of furan resin at a temperature of 1470 °C. Cylindrical rods were produced (30 mm in diameter and 100 mm in height). A combined modifier based on silicon dioxide and silicon carbide was added to the bottom of the mold cavity (additive from 0.5 to 1.5 wt. %, grain size less than 1.0 mm). Research included: determination of the chemical composition of cast iron; determination of specimens' hardness using the *Brinell* method; tensile testing of specimens; study of the macro- and microstructure of gray cast iron. The combined modifier was obtained from cyclone dust waste by flotation treatment [1, 7, 32, 33]. The appearance of the modifier is shown in figure 1, and the composition of the crystalline phase in Table 1 and figure 2. Compacting the modifier was carried out from the resulting mechanical mixtures either by tableting using a press, or a product was obtained manually globulated using paraffin. When analyzing the convex shape factor, the difference between the real and convex perimeter of the graphite particles is first determined and then the resulting value is divided by the ratio of the square root of the convex perimeter to the real perimeter of the measured particle. The roundness shape factor is commonly used to define the different morphologies of graphite in cast iron, from flake to vermicular to nodular graphite, including various subclasses for each type of graphite. The graphite roundness shape factor (*RSF*) is considered (according to the international standard *ISO 945-4-2019*) to be a characteristic of the representative morphology of graphite in cast irons. The international standard *ISO 16112:2017 "Compacted graphite cast irons – Classification"* [25] defines some of the graphite morphologies that may be present in this type of cast iron. In this *RSF* standard,

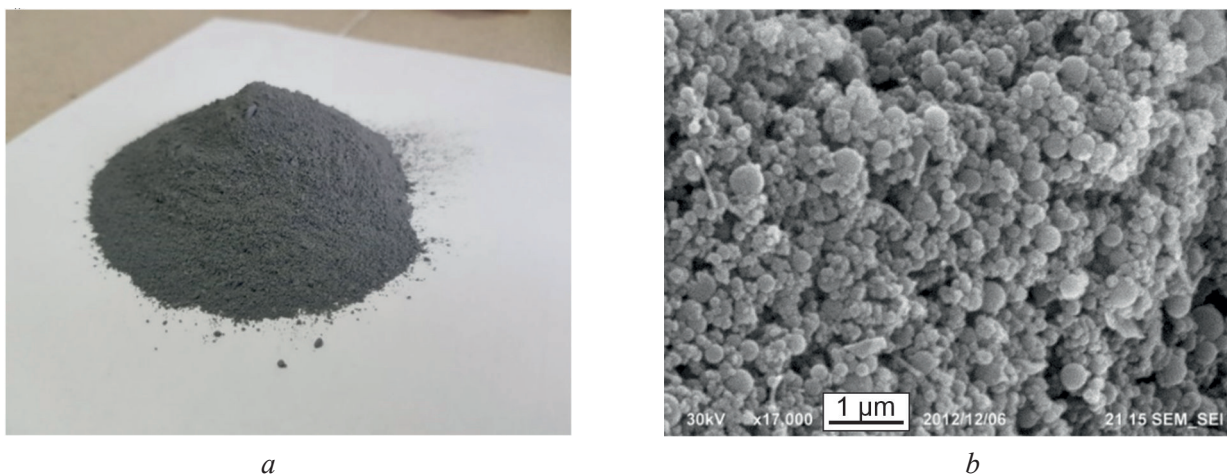


Fig. 1. The appearance of the combined modifier: formed out of silicon production waste (a); electronic photography of the structure (b)

Table 1

The composition of the crystal phase of the combined modifier according to XRD results

No.	Phase	Content (%)
1	SiO_2 (Quartz)	50
2	SiC (Moissanite)	35
3	SiO_2 (Cristobalite)	10
4	C (Graphite)	5

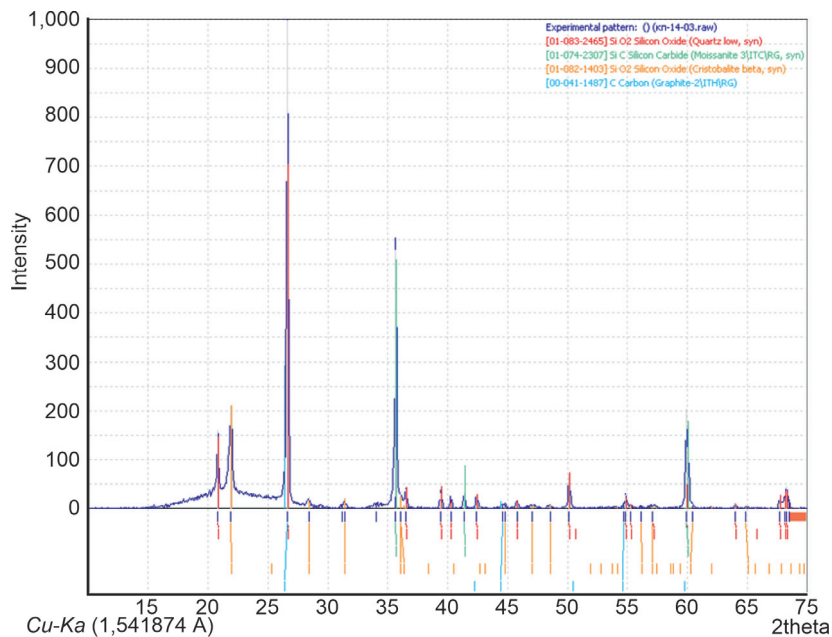


Fig. 2. Diffraction pattern of the combined modifier

nodular graphite (*ISO* Form VI) was defined using $RSF = 0.625-1.0$, with intermediate forms of graphite (*ISO* Forms IV and V) with $RSF = 0.525-0.625$ and vermicular graphite (*ISO* Form III) with $RSF < 0.525$. In our case, the graphite roundness shape factor (RSF) was in the range of $0.425-0.519$.

Results and discussion

The chemical composition of specimens of gray cast iron and with modification is presented in Table 2. It can be seen that the use of the modifier does not significantly change the chemical composition of gray cast iron, with the exception of a slight increase in silicon by 0.1 %.

It is known that for gray cast iron the main indicators of mechanical properties are the minimum value of tensile strength and hardness. Table 3 presents the results of mechanical tests of witness cast iron and specimens after modification. It can be seen that with the same chemical composition, the use of a modifier increases the mechanical properties of the casting.

The study of the macro- and microstructure of gray cast iron was carried out in accordance with *GOST 3443-87* using optical and electron microscopy, which made it possible to identify the peculiarities of the influence of modifiers. Figs. 3, 4 present the results of optical and electron microscopy. Typically, the eutectic solidification unit is represented by austenite and plate-shaped graphite (figure 3). In all cases, a predominantly lamellar structure of *Gf1* type graphite is observed according to *GOST 3443-87*. Foundry practices can influence the nucleation and growth of graphite flakes such that size and type improve

Table 2

Chemical composition of cast iron of experimental smelters No. 1 and 2 (wt. %)

Element	<i>C</i>	<i>Si</i>	<i>Mn</i>	<i>P</i>	<i>S</i>	<i>Cr</i>	<i>Ni</i>
Smelting without modifier	3.55	2.10	0.6	0.086	0.052	0.05	0.06
Smelting with modifier	3.49	2.51	0.5	0.098	0.055	0.01	0.06
Cast iron grade SCh15 (GOST 1412-85)	3.5–3.7	2.0–2.4	0.5–0.8	≤0.2	≤0.15	–	–

Table 3

Test results of a combined modifier from silicon production waste

Specimen	Modifier consumption (wt. %)	Hardness, <i>HB</i>	σ_u (MPa)	Compliance with cast iron grade
исходный	–	195; 201; 193	139; 143; 147	<i>SCh1510, SCh1515</i>
No. 1	0.5	196; 200; 198	155; 151; 149	<i>SCh1510, SCh1515</i>
No. 2	1.0	205; 208; 209	165; 174; 177	<i>SCh1520</i>
No. 3	1.5	255; 260; 258	305; 310; 312	<i>SCh1530</i>

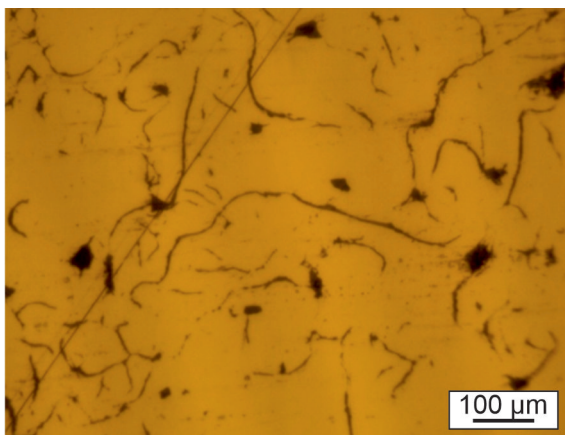
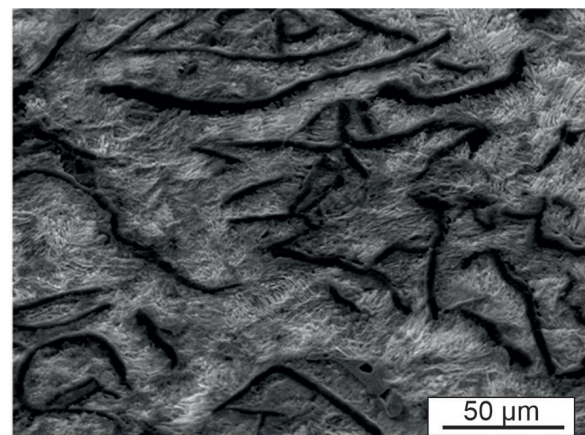
*a**b*

Fig. 3. Lamellar rectilinear form of graphite on the surface of unmodified cast iron specimens: optical (*a*) and electron (*b*) microscopy

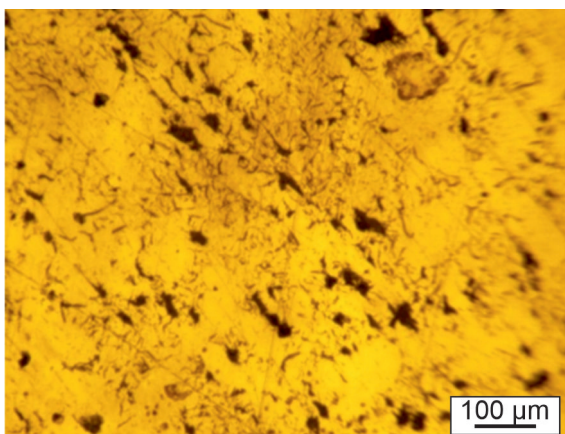
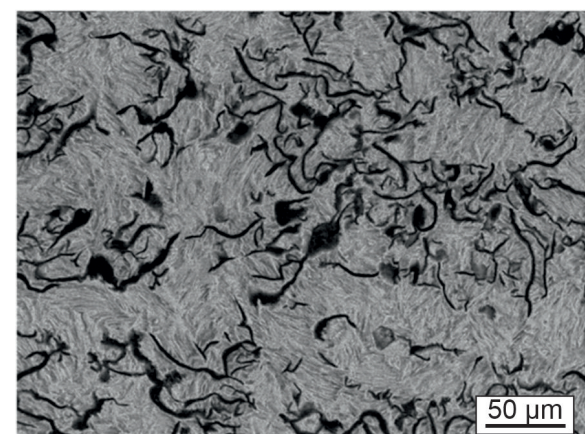
*a**b*

Fig. 4. The vermicular graphite shape of the surface of cast iron specimens after modification: optical (*a*) and electronic (*b*) microscopy

mechanical properties. The amount and size of graphite, morphology and distribution of graphite flakes are critical in determining the mechanical behavior [26–34]. Lamellar graphite of the *Gfl* type in our studies has a random orientation. As shown in figure 2, *b*, the morphology of vermicular graphite type *Gf5* was observed using optical and electron microscopy.

Figure 4 shows a large amount of vermicular graphite with uneven distribution. The ends of vermicular graphite are relatively smooth, round and blunt in shape, while the outer edge has a wavy, uneven shape. It is obvious that the graphite structures are thin and dispersed. Vermicular graphite makes up approximately 50 % of the volume, and several other graphite phases can be seen throughout the field of view. Vermicular graphite inside the eutectic cluster (figure 4, *b*) is a continuous structure with a hemispherical end. The ends of vermicular graphite between the eutectic clusters are not nested into each other and represent full-fledged and independent particles of the eutectic cluster.

Figure 4, *b* shows metallographic photographs of the core of a gray cast iron casting. The graphite morphology is fine vermicular graphite about 100–200 μm in length and only a small amount of spherical graphite. According to the requirements of regulatory documents, it is necessary to calculate each graphite morphology over the cross section of the specimen. The percentage of vermicular graphite on the surface and core of the casting is 93 % and 51 %, respectively. The matrix structure of the casting is pearlitic; a small amount of ferrite precipitates around the graphite. It was found that specially shaped graphite existed in the matrix in addition to vermicular graphite and spherical graphite, as shown in figure 4, *b*. This type of graphite morphology is presented in the form of spherical graphite with a small tail, which was called tadpole graphite (distorted graphite) in [18]. Most of the distorted graphite head has an irregular spherical shape, with a diameter of about 20–50 μm , and a tail length of about 30–120 μm . Interestingly, the graphite tail in some areas is separated from the parent body of spherical graphite. The morphology of distorted graphite is between spheroidal graphite and vermicular graphite, which is not yet fully developed.

When analyzing the results (Table 2, 3), it is clear that the combined modifier demonstrates good modifying properties. The modified specimens showed higher mechanical properties compared to the witness sample. Previously, in [7, 32, 33], we compared modifiers consisting of silicon dioxide with the standard modifier *FS75*, which showed an increase in the positive effect on the structure and properties. From the theory and practice of foundry production it is known that the effectiveness of modification in the smelting of gray cast iron is checked when processing cast iron with a low carbon equivalent. This study shows that the combined modifier has a positive effect on the mechanical properties of gray cast iron.

On specimens without modification (figure 3), we see that graphite has a morphological shape in the form of plates. Vermicular graphite (figure 4) is a transitional form between flake graphite and spherical graphite [8–19], and its roundness factor (*RSF*) ranges from 0.3 to 0.6. The roundness coefficient was calculated according to the formulas [23, 25]. The morphology of graphite plays an important role in the mechanical properties of gray cast irons. According to the theory of cast iron crystallization, the final shape of graphite is uncontrollable at the nucleation stage and depends on the growth stage. The differences in graphite morphology are due to different growth rates in all directions. The direction of growth depends mainly on the chemical composition [17–21]. The differences in the growth behavior of lamellar, spherical and vermicular graphite depend mainly on the exclusion of selective adsorption of surface-active atoms on the graphite surface [18]. During eutectic cluster growth, low melting point and low content compounds such as sulfur and phosphorus are typically thrown to the grain boundaries, and austenite does not surround the vermicular graphite during growth. As graphite solidifies, it is able to change the direction of its growth at the solid-liquid interface.

During the solidification process of cast iron, the mode of graphite growth and the final morphology depend on the thermodynamic conditions and chemical composition of the molten cast iron. According to works [8–19, 26–39], the mechanism of formation of graphite morphology in cast iron is as follows. When the molten iron is sufficiently pure and free of surfactants (*O*, *S* or other impurities), the main growth direction of graphite is the normal of the basal plane (0001) (*c* direction), and the graphite will preferentially develop through spiral growth into a spherical shape, since it can occur with minimal activation energy [20, 21]. However, molten iron inevitably contains surfactants such as *S* and *O*, which have been found



[8–13] to be absorbed at graphite-iron interfaces and are likely to increase the undercooling required for growth, especially at the hexagonal facet plane. graphite lattice shapes. As a result, the direction of graphite growth changes to normal to the plane of the face (a-direction) and lamellar graphite is formed [1, 15-18]. Therefore, when producing compacted graphite cast iron, elements (*Mg, La, Ce*, etc.) are usually added to consume the surfactants around the graphite. As a result, graphite grows alternately in the a direction and then in the c direction, forming vermicular graphite [8–11]. In our case, compounds of silicon dioxide and silicon carbide perform the same roles, which leads to a change in the morphology of graphite in gray cast iron.

It is important to note that for decades, graphite shapes in cast iron have been assessed by comparing microscopic images to stylized reference images, with a preferred magnification of 100× [23–25]. Two different approaches to graphite classification have been standardized by *ISO* and *ASTM* (see figure 5) and the domestic standard [24], which differ in the number, name and examples of graphite particles depicted (figure 5). However, when analyzing foreign and domestic standards, all evaluation approaches subjectively change the shape of graphite from lamellar to nodular with some more or less degenerate shapes in between.

In figure 5, we took the requirements for graphite morphology from each standard and combined them in one drawing. The domestic standard [24] contains more than 13 types of graphite morphology and is designated by the letters *Γ* with the corresponding index.

For example [22–25], the *EN ISO 945-1* defined **VI ISO** and **V ISO** shapes can be considered similar to *ASTM I ASTM* and *II ASTM* shapes, although *II ASTM* are convex particles whereas **V ISO** shape appears more star-shaped. Both forms contain the desired round particles as well as less round particles that are not likely to affect the mechanical properties. **IV ISO** and *III ASTM* forms contain particles that are common in ductile iron, but the forms presented are different. **IV ISO** and *III ASTM* forms are compacted particles that are desirable in ductile iron and may also be found in nodular cast iron. **II ISO** form is a stylized representation of degenerated graphite particles known as pointed or intercellular graphite, which is mainly formed from trace elements. Unlike its stylistic image, this form does not appear independently, but

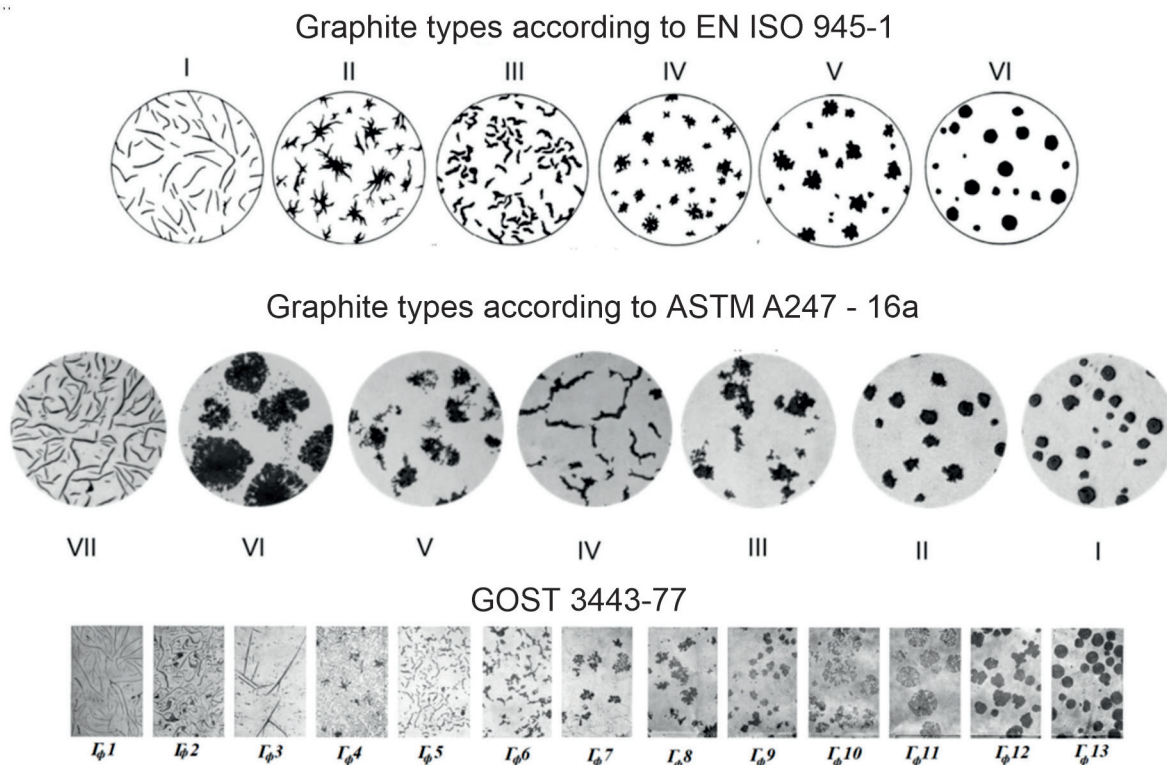


Fig. 5. Various standard approaches to graphite classification:
 upper row: graphite types in accordance with *EN ISO 945-1*, middle row: graphite types in accordance with *ASTM A247 – 16a*, lower row: graphite types in accordance with *GOST 3443-77*



only in combination with spherical or flake graphite. In contrast, **V ASTM** form is an actual microscopic image of degenerated graphite, which has a very different appearance **II ISO** from. Although **VI ASTM** form shows an example of blasted graphite, *EN ISO 945-1* does not provide reference pictures for these types of graphite degeneration. Both *ASTM A247* and *EN ISO 945-1* represent flake graphite (**I ISO** and **VII ASTM**) in the same way. In addition to stylistic illustrations, *EN ISO 945-1* also contains actual microscopic examples of **I ISO** Forms and **III–VI ISO**. In *GOST 3443-87*, flake graphite is represented by $\Gamma_{\phi}1$ – $\Gamma_{\phi}4$, vermicular $\Gamma_{\phi}5$, $\Gamma_{\phi}6$. According to the requirements of *GOST 3443-77*, during the analysis process, in the case of a pronounced mixed morphology of graphite, it is necessary to carry out a manual analysis of each structural component (lamellar, vermicular, spherical), which is associated with high labor intensity of the analysis and subjective interpretation of the results.

In *GOST 3443-87*, lamellar graphite is represented by $\Gamma_{\phi}1$ – $\Gamma_{\phi}4$, vermicular $\Gamma_{\phi}5$, $\Gamma_{\phi}6$. According to the requirements of *GOST 3443-87*, during the analysis process, in the case of a pronounced mixed morphology of graphite, it is necessary to carry out a manual analysis of each structural component (lamellar, vermicular, spherical), which is associated with high labor intensity of the analysis and subjective interpretation of the results.

In [35–38], a new approach to the instrumental assessment of the morphological features of graphite during crystallization is presented based on thermal analysis combined with an assessment of expansion and contraction during cooling. A mechanical expansion/contraction system was used to evaluate the initial expansion of magnesium-treated cast irons, which was identified as the main factor influencing the shrinkage sensitivity of cast irons with different graphite morphologies [36]. It was found (figure 6) [39] that the formation of graphite led to an important event at the onset of solidification, namely initial expansion in all cast irons containing graphite, due to the force generated by the formation of different graphite morpholo-

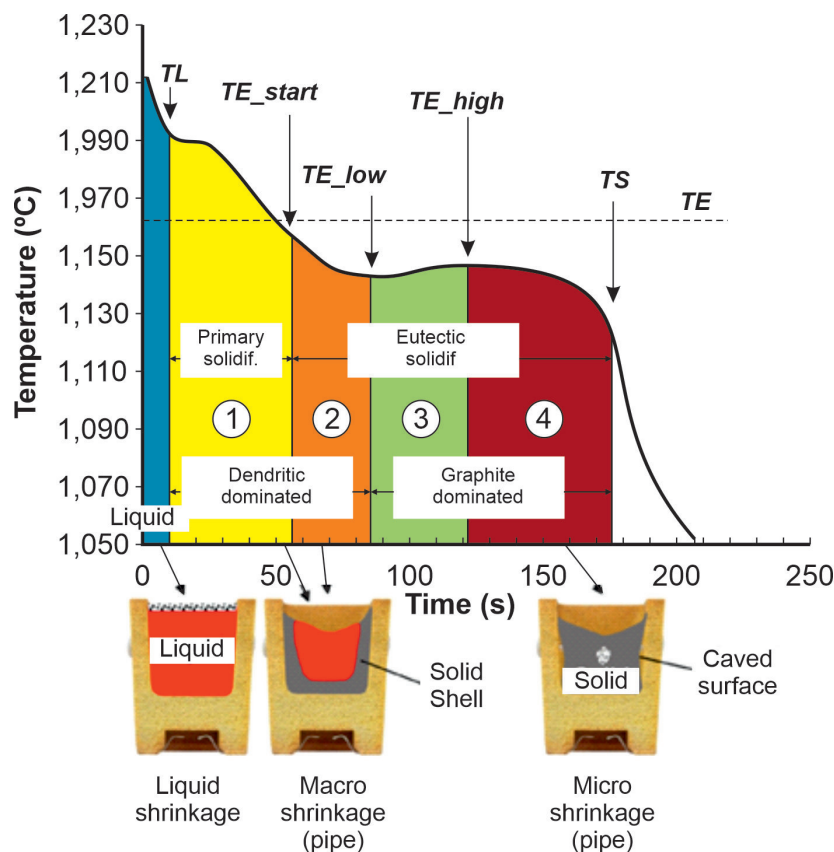


Fig. 6. The cooling curve of pre-eutectic cast iron with characteristic temperatures showing the solidification intervals of the primary and eutectic phases and the correlation with the formation of shrinkage defects [39]

gies applied to the mold wall [35, 36]. Liquid iron begins to cool and shrink immediately after pouring. The density of the liquid increases and the specific volume decreases, which leads to shrinkage of the liquid. This shrinkage can be compensated for by risers. According to [39], in iron, solidification then begins at the liquidus temperature (TL) with the formation of dendrites that grow inward from the walls of the cup until eutectic solidification begins (zone 1 in figure 6). Dendritic shrinkage can continue even after solidification has begun (TE_{start}), since the amount of eutectic formed is initially small (zone 2). As long as the supply channel is open and the permeability of the loose dendritic region is sufficiently high, the shrinkage is compensated by the flow from the risers. After reaching maximum supercooling (TE_{low}), the rapid formation of eutectic shifts the emphasis of solidification from the predominance of dendritic shrinkage (zones 1 and 2) to the predominance of graphitic expansion (zones 3 and 4).

The expansion of graphite may or may not continue until the end of solidification [39]. In zone 3, sufficient expansion of the graphite compensates for the compression of the liquid and dendrites. In zone 4, when the amount of eutectic formed and therefore graphite decreases, there is a risk of micro-shrinkage (microporosity) as the expansion of graphite may become insufficient to compensate for the shrinkage. In principle, both LG and SG cast irons are close to eutectic in composition and should exhibit expansion during solidification, hence should not be prone to cavity formation or shrinkage of porosity. Although this is true for gray cast iron, conventionally produced nodular iron is subject to shrinkage porosity.

For nodular cast iron, the melting zone is much larger and its permeability is much less than that of flake graphite cast iron. This, according to [39], limits the flow from the riser and reduces the cooling rate. Due to the limited growth of graphite at the end of solidification, austenite shrinkage predominates, which causes a decrease in the specific volume and leads to uncompensated shrinkage in the last solidification zone. This effect and the significant release of gas from the solidifying liquid lead to the formation of porosity. Experimental linear displacement analysis (LDA) and thermal analysis (TA) devices have been used by a number of researchers [7–21] to measure the amplitude of the expansion/contraction effects occurring during the solidification of cast iron. An extensive literature review on various methods was provided in [35].

A setup for thermal analysis was previously presented by us in [7]. In addition to this, a stand was developed that includes two parallel molds for pouring specimens (mold sizes 200 mm and 30 mm), a cooling module (0.72 cm) and a deformation recording module. The high-speed interface simultaneously records temperature and linear displacement data. The results of preliminary experiments are shown in figure 7. The morphology of graphite has a marked influence on the initial expansion value: it increases from flake graphite (LG) through vermicular graphite (CG) to nodular graphite (NG), respectively. In the same way, sensitivity to shrinkage increases, and the connection between two parameters is obvious: initial expansion - level of shrinkage. These experiments also demonstrated the importance of accurately estimating contraction/expansion events and their relationship to cooling curve events, respectively.

Several key parameters have been identified that correlate with the specific behavior of our inoculants as it relates to graphite release and shrinkage sensitivity of gray cast iron. These were: depth of eutectic supercooling, recalescence and maximum recalescence rate, temperature of the end of solidification, maximum initial expansion and the total integral from the first derivative of the compression curve to the end of pre-pearlite compression. Subcooling at the end of solidification relative to the metastable (carbide)

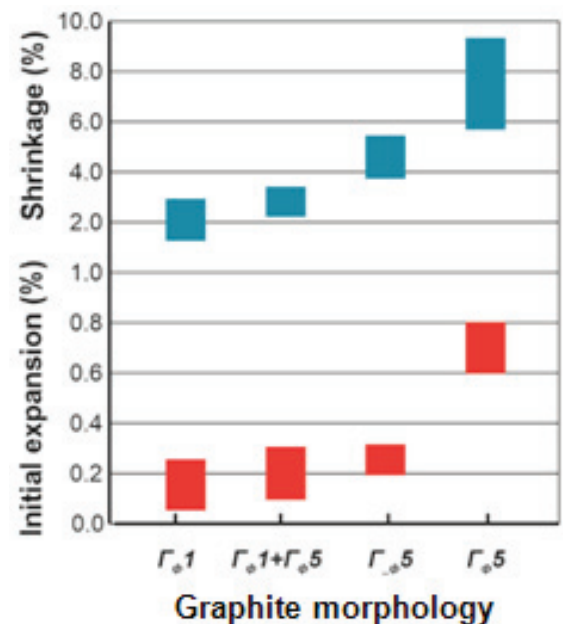


Fig. 7. The results of the study of the influence of graphite morphology on the initial expansion (compression curve) and the tendency to shrinkage ($\Gamma_{\phi 1}$ – lamellar, $\Gamma_{\phi 5}$ – vermicular)

equilibrium temperature and expansion within the solidification sequence appear to have a strong influence [39] on the susceptibility to macro- and micro-shrinkage in ductile iron castings.

The work [34] states that molten cast iron usually contains double oxide films (bifilms). These silicate oxide films provide a substrate on which oxysulfides and graphite nuclei form. The presence of these double silicate films explains the diversity of graphite morphology.

Lamellar graphite grows along the films, and spherical graphite grows when these films are destroyed, for example, with the addition of magnesium. It was shown in [10–17, 35–39] that the appearance of the vermicular form of graphite was associated not only with the interaction of silicon with carbon monoxide, but also due to the interaction, in this case, of silicon monoxide with a graphite nucleus. As the temperature of the metal melt decreases, the surface activity of SiO decreases [10–12], its mobility decreases, and at the site of formation it dissolves in graphite, changing its morphology to vermicular [35–39].

In conclusion, we note that the components of the combined modifier (silicon oxides and carbides) do not dissolve immediately when added to the melt; dissolution occurs slowly, which gives a preliminary inoculation effect that slowly fades and remains effective for several hours [8, 12–15, 26, 28, 34–42]. At the same time, the behavior of SiC before modification in gray cast iron melts has not been sufficiently studied, but it is stated [31, 41, 42] that during the dissolution of SiC in the melt, graphite clusters form around SiC particles as a result of local supersaturation of the melt with Si and C . These graphite clusters, which are thermodynamically metastable over a period of time, play an important role in the pre-modification effect of SiC in the melt and promote the formation of graphite and eutectic nucleation. Dissolution of the $FeSi$ compound can also result in the formation of graphite clusters, but due to the higher dissolution rate these clusters remain stable only for short periods of time. Consequently, when SiC is dissolved, more graphite clusters are formed, which last longer than when $FeSi$ is dissolved. The formation of many graphite clusters around the SiC particles reduces the carbon content in the rest of the melt, and therefore austenite nucleation occurs at higher temperatures. The use of modifiers from silicon production waste to achieve the technological properties of gray cast iron together with other advanced technologies in mechanical engineering and metal processing [43–50] will make it possible to comprehensively solve high-tech, knowledge-intensive problems.

Conclusions

1. Studies conducted to assess the modifying effect of a combined modifier obtained from silicon production waste in the smelting of gray cast iron show its high efficiency compared to classical modifiers. It is established that the addition of a combined modifier based on silicon oxide and carbide instead of the standard $FeSi$ modifier led to an increase in tensile strength and hardness by 35–50%, due to a change in the morphology of graphite from lamellar to vermicular.

2. It is shown that the proposed composition of the combined modifier induces the nucleation of a large amount of vermicular graphite, and also increases the number of eutectic cells and reduced the tendency to form white cast iron.

3. It is shown that the analysis of compression/expansion effects during the crystallization process correlates well with the change in solidification parameters in accordance with the characteristics of the molten cast iron, which depend on the melting procedure and the modifiers used, the rigidity of the mold and thermal behavior (heat transfer parameters).

References

1. Kondrat'ev V.V., Balanovskii A.E., Ivanov N.A., Ershov V.A., Korniyakov M.V. Evaluation of the effect of modifier composition with nanostructured additives on grey cast iron properties. *Metallurgist*, 2014, vol. 58, pp. 377–387. DOI: 10.1007/s11015-014-9919-x.
2. Kondrat'ev V.V., Mekhnin A.O., Ivanov N.A., Bogdanov Yu.V., Ershov V.A. Issledovaniya i razrabotka retseptury nanomodifitsirovannogo chuguna dlya nippelei anodov alyuminievykh elektrolizerov [Research and development of



composition of nano-inoculated cast iron for anodes stubs of aluminium pots]. *Metallurg = Metallurgist*, 2012, no. 1, pp. 69–71. (In Russian).

3. Kondratyev V.V., Nemchinova N.V., Ivanov N.A., Ershov V.A., Sysoev I.A. Novye tekhnologicheskie resheniya po pererabotke otkhodov kremnievogo i alyuminievogo proizvodstv [New production solutions for processing silicon and aluminum production waste]. *Metallurg = Metallurgist*, 2013, no. 5, pp. 92–95. (In Russian).

4. Evseev N.V., Tyutrin A.A., Pastukhov M.P. Granulirovanie pylevykh otkhodov kremnievogo proizvodstva dlya vozvrata v tekhnologicheskii protsess [Granulation of silicone production dust waste for recycling]. *Vestnik Irkutskogo gosudarstvennogo tekhnicheskogo universiteta = Proceedings of Irkutsk State Technical University*, 2019, vol. 23 (4), pp. 805–815. DOI: 10.21285/1814-3520-2019-4-805-815.

5. Babkov V.V., Gabitov A.I., Sakhibgareev P.P. Amorfnyi mikrokremnezem v protsessakh strukturoobrazovaniya i uprochneniya tsementnogo kamnya [Amorphous microsilica in structurization and hardening of a cement stone processes]. *Bashkirskii khimicheskii zhurnal = Bashkir Chemical Journal*, 2007, vol. 17 (3), pp. 206–210.

6. AlTawaiha H., Alhomaidat F., Eljufout T. A review of the effect of nano-silica on the mechanical and durability properties of cementitious composites. *Infrastructures*, 2023, vol. 8 (9), p. 132. DOI: 10.3390/infrastructures8090132.

7. Karlina A.I. *Tekhnologiya pererabotki pyli gazoochistki prizvodstva kremniya v modifitsiruyushchie nanodobavki dlya chugunov*. Avtoref. diss. kand. tekhn. nauk [Technology of processing gas purification dust from silicon production into modifying nanoadditives for cast iron. Author's abstract of PhD eng. sci. diss.]. Ekaterinburg, 2019. 24 p.

8. Stefanescu D.M., Alonso G., Larrañaga P., De la Fuente E., Suarez R. Reexamination of crystal growth theory of graphite in iron-carbon alloys. *Acta Materialia*, 2017, vol. 139, pp. 109–121. DOI: 10.1016/j.actamat.2017.08.004.

9. Riposan I., Chisamera M., Stan S., Hartung C., White D. Three-stage model for nucleation of graphite in grey cast iron. *Materials Science and Technology*, 2010, vol. 26 (12), pp. 1439–1447. DOI: 10.1179/026708309X12495548508626.

10. Stefan E., Riposan I., Chisamera M. Application of thermal analysis in solidification pattern control of La-inoculated grey cast irons. *Journal of Thermal Analysis and Calorimetry*, 2019, vol. 138, pp. 2491–2503. DOI: 10.1007/s10973-019-08714-7.

11. Riposan I., Stefan E., Stan S., Pana N.R., Chisamera M. Effects of inoculation on structure characteristics of high silicon ductile cast irons in thin wall castings. *Metals*, 2020, vol. 10 (8), p. 1091. DOI: 10.3390/met10081091.

12. Riposan I., Skaland T. Modification and inoculation of cast iron. *Cast Iron Science and Technology Handbook*. ASM International, 2017, pp. 160–176. DOI: 10.31399/asm.hb.v01a.a0006315.

13. Anca D.-E., Stan I., Riposan I., Stan S. Graphite compactness degree and nodularity of high-Si ductile iron produced via permanent mold versus sand mold casting. *Materials*, 2022, vol. 15, p. 2712. DOI: 10.3390/ma15082712.

14. Sommerfeld A., Tonn B. Theory of graphite nucleation in lamellar graphite cast iron. *International Journal of Metalcasting*, 2009, vol. 3, pp. 39–47. DOI: 10.1007/BF03355457.

15. Double D.D., Hellawell A. The nucleation and growth of graphite—the modification of cast iron. *Acta Metallurgica et Materialia*, 1995, vol. 43 (6), pp. 2435–2442. DOI: 10.1007/BF03355457.

16. Amini S., Garay J., Liu G., Balandin A.A., Abbaschian R. Growth of large-area graphene films from metal-carbon melts. *Journal of Applied Physics*, 2010, vol. 108 (9), pp. 094321–094327. DOI: 10.1063/1.3498815.

17. Amini S., Kalaantari H., Garay J., Balandin A.A., Abbaschian R. Growth of graphene and graphite nanocrystals from a molten phase. *Journal of Materials Science*, 2011, vol. 46 (19), pp. 6255–6263. DOI: 10.1007/s10853-011-5432-9.

18. Stefanescu D.M., Alonso G., Larrañaga P., De la Fuente E., Suárez R. On the crystallization of graphite from liquid iron-carbon-silicon melts. *Acta Materialia*, 2016, vol. 107, pp. 102–126. DOI: 10.1016/j.actamat.2016.01.047.

19. Qing J., Lekakh S., Xu M., Field D. Formation of complex nuclei in graphite nodules of cast iron. *Carbon*, 2021, vol. 171, pp. 276–288. DOI: 10.1016/j.carbon.2020.08.022.

20. Theuwissen K., Lacaze J., Laffont L. Structure of graphite precipitates in cast iron. *Carbon*, 2016, vol. 96, pp. 1120–1128. DOI: 10.1016/j.carbon.2015.10.066.

21. Amini S., Abbaschian R. Nucleation and growth kinetics of graphene layers from a molten phase. *Carbon*, 2013, vol. 51, pp. 110–123. DOI: 10.1016/j.carbon.2012.08.019.

22. ASTM A247-67(1998)e1. *Standard test method for evaluating the microstructure of graphite in iron castings*. West Conshohocken, PA, ASTM International, 1967.

23. DIN EN ISO 945-1–2019. *Microstructure of cast irons – Part 1: Graphite classification by visual analysis (ISO 945-1:2019)*. German version EN ISO 945-1:2019. 40 p.



24. GOST 3443–87. *Otlivki iz chuguna s razlichnoi formoi grafita. Metody opredeleniya struktury* [State Standard. Cast iron castings with graphite of different form. Methods of structure determination]. Moscow, Standards Publ., 2003. 42 p.
25. ISO 16112:2006. *Compacted (vermicular) graphite cast irons – Classifications*. Switzerland, International Organization for Standardization, 2006. 23 p.
26. König M. Literature review of microstructure formation in compacted graphite Iron. *International Journal of Cast Metals Research*, 2010, vol. 23 (3), pp. 185–192. DOI: 10.1179/136404609X12535244328378.
27. König M., Wessén M. Influence of alloying elements on microstructure and mechanical properties of CGI. *International Journal of Cast Metals Research*, 2010, vol. 23 (2), pp. 97–110. DOI: 10.1179/136404609X12505973098972.
28. Stefanescu D.M., Alonso G., Suarez R. Recent developments in understanding nucleation and crystallization of spheroidal graphite in iron-carbon-silicon alloys. *Metals*, 2020, vol. 10, p. 221. DOI: 10.3390/met10020221.
29. Lacaze J., Castro-Roman M.J. Comment on Stefanescu, D.M.; Alonso, G.; Suarez, R. Recent developments in understanding nucleation and crystallization of spheroidal graphite in iron-carbon-silicon alloys. *Metals* 2020, 10, 221. *Metals*, 2020, vol. 10 (4), p. 471. DOI: 10.3390/met10040471.
30. Chen Y., Pang J.C., Li S.X., Zou C.L., Zhang Z.F. Damage mechanism and fatigue strength prediction of compacted graphite iron with different microstructures. *International Journal of Fatigue*, 2022, vol. 164, p. 107126. DOI: 10.1016/j.ijfatigue.2022.107126.
31. Zykova A.P., Lychagin D.V., Chumaevskii A.V., Kurzina I.A., Novomeiskii M.Yu. Vliyanie modifitsirovaniya ul'tradispersnymi poroshkami oksidov tugoplavkikh metallov i kriolita na strukturu, mekhanicheskie svoistva i razrushenie chuguna SCh25 [Influence of modifying of cast iron SCh25 (Russian grade) with ultrafine powders of refractory metal oxide and cryolite on structure, mechanical properties and fracture]. *Izvestiya vysshikh uchebnykh zavedenii. Chernaya metallurgiya = Izvestiya. Ferrous Metallurgy*, 2014, vol. 57 (11), pp. 37–42. DOI: 10.17073/0368-0797-2014-11-37-42. (In Russian).
32. Kondratyev V.V., Ivanov N.A., Balanovskiy A.E., Ivanchik N.N., Karlina A.I. Uluchshenie svoistv serogo chuguna kremniidioksid i uglerodnymi nanostrukturami [Improvement of the properties of gray cast iron by silicon dioxide and carbon nanostructures]. *Zhurnal Sibirskogo federal'nogo universiteta. Seriya: Tekhnika i tekhnologii = Journal of Siberian Federal University. Engineering & Technologies*, 2016, vol. 9 (5), pp. 671–685. DOI: 10.17516/1999-494X-2016-9-5-671-685.
33. Kondratyev V.V., Balanovskiy A.E., Ivanov N.A., Ershov V.A., Korniyakov M.V. Otsenka vliyaniya sostava modifikatora s nanostrukturnymi dobavkami na svoistva serogo chuguna [Impact assessment of modifier composition with nanostructured additives on properties of grey cast iron]. *Metallurg = Metallurgist*, 2014, no. 5, pp. 48–56.
34. Boldirev D.A., Chaykin V.A., Chaykin A.B. Primenenie smesevykh kompleksnykh modifikatorov s kal'tsiistrontsievym karbonatom pri poluchenii otlivok detalei legkovogo avtomobilya iz vysokoprochnogo i serogo chugunov [Usage of mixed complex inoculators with calcium_strontium carbonate in auto_mobile casting production of nodular and gray cast iron]. *Liteishchik Rossii = Foundrymen of Russia*, 2010, no. 1, pp. 21–26.
35. Svidró P., Diószegi A. On problems of volume change measurements in lamellar cast iron. *International Journal of Cast Metals Research*, 2014, vol. 27 (1), pp. 26–37. DOI: 10.1179/1743133613Y.0000000075.
36. Cao M., Baxevanakis K.P., Silberschmidt V.V. Effect of graphite morphology on the thermomechanical performance of compacted graphite iron. *Metals*, 2023, vol. 13, p. 473. DOI: 10.3390/met13030473.
37. Stan S., Chisamera M., Riposan I., Neacsu L., Cojocaru A.M., Stan I. Integrated system of thermal/dimensional analysis for quality control of metallic melt and ductile iron casting solidification. *Journal of Materials Engineering and Performance*, 2018, vol. 27, pp. 5187–5196. DOI: 10.1007/s11665-018-3303-0.
38. Xijun D., Peiyue Z., Qifu L. Structure and formation of vermicular graphite. *MRS Online Proceedings Library*, 1984, vol. 34, pp. 141–150. DOI: 10.1557/PROC-34-141.
39. Stefanescu D.M., Suarez R., Kim S.B. 90 years of thermal analysis as a control tool in the melting of cast iron. *China Foundry*, 2020, vol. 17, pp. 69–84. DOI: 10.1007/s41230-020-0039-x.
40. Alonso G., Stefanescu D.M., Sanchez J., Zarrabeitia G., Suarez R. Effect of the type of inoculant on the shrinkage porosity of high-silicon SG iron. *International Journal of Metalcasting*, 2022, vol. 16, pp. 106–118. DOI: 10.1007/s40962-021-00605-8.
41. Cherepanov A.N., Drozdov V.O., Manolov V.K., Poluboyarov V.A. Vliyanie nanoporoshkov tugoplavkikh soedinenii na svoistva serogo chuguna [The influence of nanopowders of refractory compounds on the properties of gray cast iron]. *Tyazheloe mashinostroenie*, 2012, no. 8, pp. 8–11. (In Russian).



42. Krushenko G.G., Yamskikh I.S., Bonchenkov A.A., Mishin A.S. Povyshenie kachestva chugunnykh otlivok s pomoshch'yu nanoporoshkov [Improving the quality of cast iron castings using nanopowders]. *Metallurgiya mashinostroeniya = Metallurgy of machinery building*, 2002, no. 2 (9), pp. 20–21.

43. Skeebe V.Yu., Ivancivsky V.V., Kutyshkin A.V., Parts K.A. Hybrid processing: the impact of mechanical and surface thermal treatment integration onto the machine parts quality. *IOP Conference Series: Materials Science and Engineering*, 2016, vol. 126 (1), p. 012016. DOI: 10.1088/1757-899x/126/1/012016.

44. Efremkov E.A., Martyushev N.V., Skeebe V.Yu., Grechneva M.V., Olisov A.V., Ens A.D. Research on the possibility of lowering the manufacturing accuracy of cycloid transmission wheels with intermediate rolling elements and a free cage. *Applied Sciences*, 2022, vol. 12 (1), p. 5. DOI: 10.3390/app12010005.

45. Martyushev N.V., Skeebe V.Yu. The method of quantitative automatic metallographic analysis. *Journal of Physics: Conference Series*, 2017, vol. 803 (1), p. 012094. DOI: 10.1088/1742-6596/803/1/012094.

46. Skeebe V.Yu., Ivancivsky V.V. Reliability of quality forecast for hybrid metal-working machinery. *IOP Conference Series: Earth and Environmental Science*, 2018, vol. 194 (2), p. 022037. DOI: 10.1088/1755-1315/194/2/022037.

47. Zverev E.A., Skeebe V.Yu., Skeebe P.Yu., Khlebova I.V. Defining efficient modes range for plasma spraying coatings. *IOP Conference Series: Earth and Environmental Science*, 2017, vol. 87 (8), p. 082061. DOI: 10.1088/1755-1315/87/8/082061.

48. Skeebe V.Yu. Gibridnoe tekhnologicheskoe oborudovanie: povyshenie effektivnosti rannikh stadii proektirovaniya kompleksirovannykh metalloobratyvyayushchikh stankov [Hybrid process equipment: improving the efficiency of the integrated metalworking machines initial designing]. *Obrabotka metallov (tekhnologiya, oborudovanie, instrumenty) = Metal Working and Material Science*, 2019, vol. 21 (2), pp. 62–83. DOI: 10.17212/1994-6309-2019-21.2-62-83.

49. Borisov M.A., Lobanov D.V., Yanyushkin A.S., Skeebe V.Yu. Issledovanie protsessa avtomaticheskogo upravleniya smenoi polyarnosti toka v usloviyakh gibridnoi tekhnologii elektrokhimicheskoi obrabotki korroziionostoikikh stalei [Investigation of the Process of Automatic Control of Current Polarity Reversal in the Conditions of Hybrid Technology of Electrochemical Processing of Corrosion-Resistant Steels]. *Obrabotka metallov (tekhnologiya, oborudovanie, instrumenty) = Metal Working and Material Science*, 2020, vol. 22 (1), pp. 6–15. DOI: 10.17212/1994-6309-2020-22.1-6-15.

50. Mamadaliev R.A., Bakhmatov P.V., Martyushev N.V., Skeebe V.Yu., Karlina A.I. Influence of welding regimes on structure and properties of steel 12KH18N10T weld metal in different spatial positions. *Metallurgist*, 2022, vol. 65 (11–12), pp. 1255–1264. DOI: 10.1007/s11015-022-01271-9.

Conflicts of Interest

The authors declare no conflict of interest.

© 2024 The Authors. Published by Novosibirsk State Technical University. This is an open access article under the CC BY license (<http://creativecommons.org/licenses/by/4.0>).

